Supplementary Materials: Crystal Structure and Magnetic Properties of Peacock–Weakley Type Polyoxometalates Na$_9$[Ln(W$_5$O$_{18}$)$_2$] (Ln = Tm, Yb): Rare Example of Tm(III) SMM

Oleksandra Yu. Mariichak, Sandra Kaabel, Yevgen A. Karpichev, Georgiy M. Rozantsev, Serhii V. Radio, Céline Pichon, Hélène Bolvin and Jean-Pascal Sutter
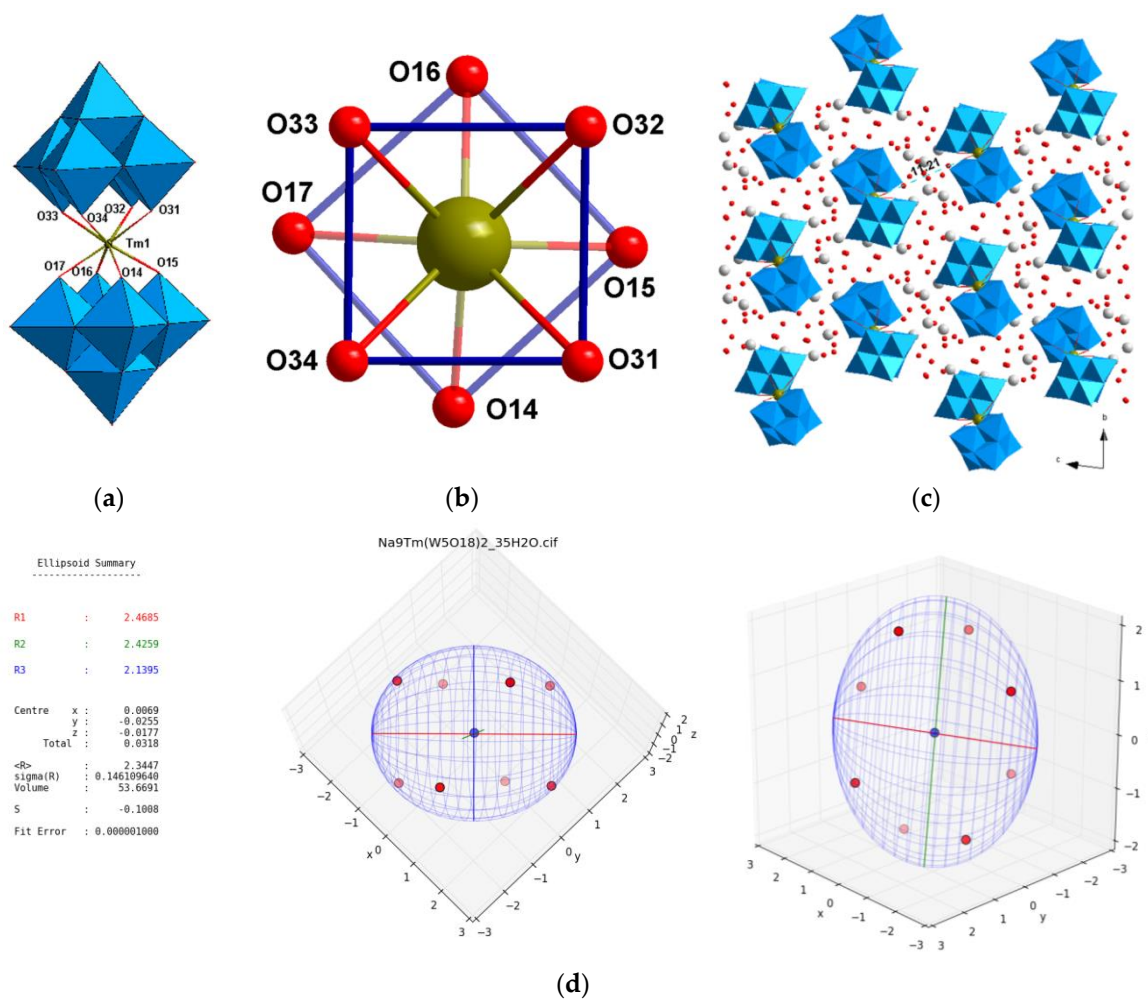

(**a**) (**b**) (**c**)

(**d**)

Figure S1. (**a**) Molecular structure of Na$_9$[Tm(W$_5$O$_{18}$)$_2$]·35H$_2$O, **1** with mixed polyhedral and ball and stick representation with thermal ellipsoids fixed at 50%. (**b**) Perspective showing the square-antiprismatic geometry around the lanthanide. (**c**) Crystal packing of **1** in the (*b*,*c*) plane. The dashed cyan line indicates the shortest Ln···Ln interaction indicated in Å. Color scheme: WO$_6$ = blue polyhedral, W = blue, Tm = bronze and O = red. (**d**) Minimum bonding ellipsoid [1] showing the oblate environment defined by the axially compressed O$_8$ coordination core Red dots materialize the coordinated O-atoms; the center and right views have orientations like in (a) and (b), respectively. R1-R3 are the principal ellipsoid radii, the negative ellipsoid shape value, S, is indicative of an oblate (axially compressed) ellipsoid.
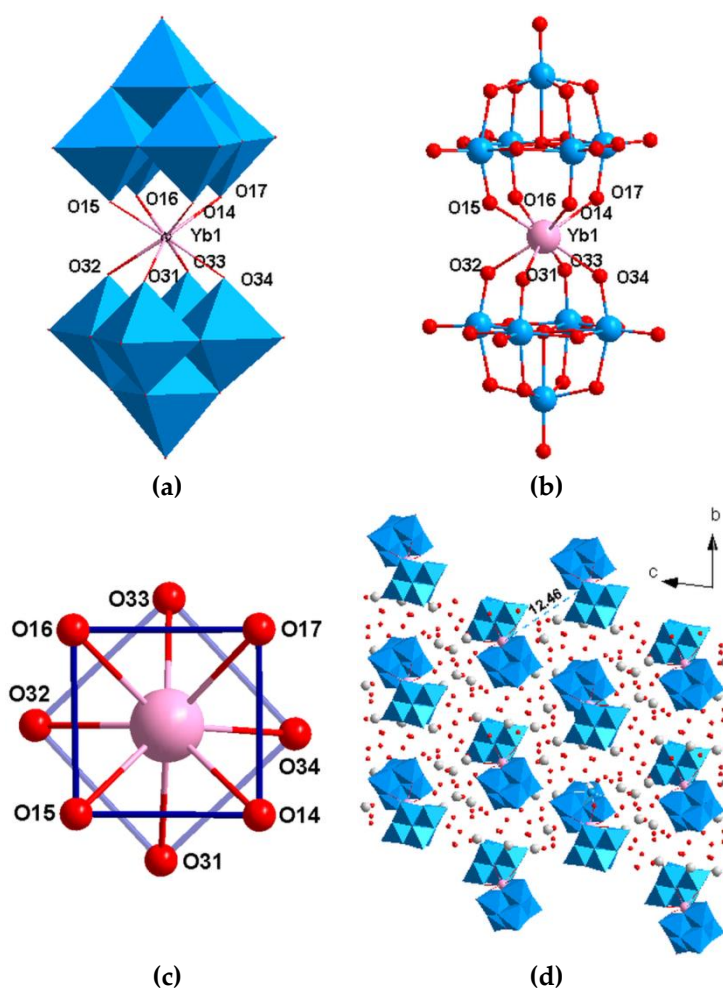
(a)   (b)

(c)   (d)

Figure S2. (**a**) Mixed polyhedral and ball and stick representation with thermal ellipsoids fixed at 50% and (**b**) ball and stick representation of the molecular structure of $Na_9[Yb(W_5O_{18})_2]\cdot35H_2O$, **2**. (**c**) Perspective showing the square-antiprismatic geometry around the lanthanide. (**d**) Crystal packing of **2** in the (*b*,*c*) plane. The dashed cyan line indicates the shortest Ln⋯Ln interaction indicated in Å. Color scheme: WO_6 = blue polyhedral, W = blue, Yb = pink and O = red.
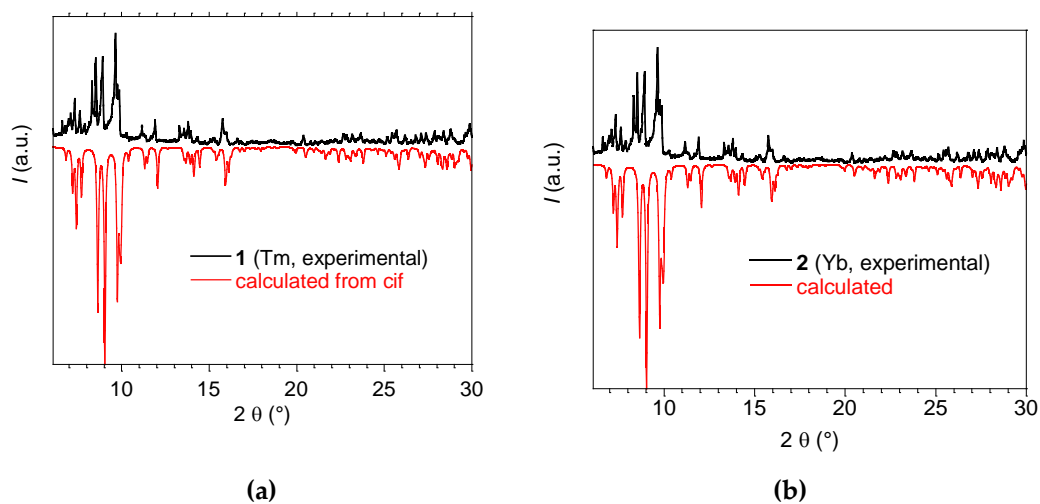
(a)　　　　　　　　　　　　(b)

Figure S3. Powder X-Ray diffractograms of **1** (**a**) and **2** (**b**). AC susceptibility investigations for $Na_9[Tm(W_5O_{18})_2]\cdot35H_2O$, **1**.

AC Susceptibility Investigations for $Na_9[Tm(W_5O_{18})_2]\cdot35H_2O$, 1:
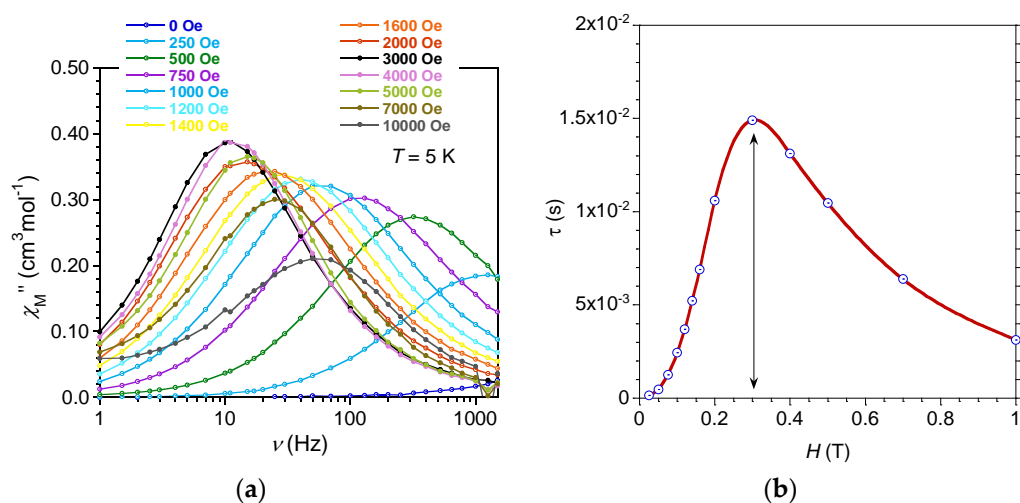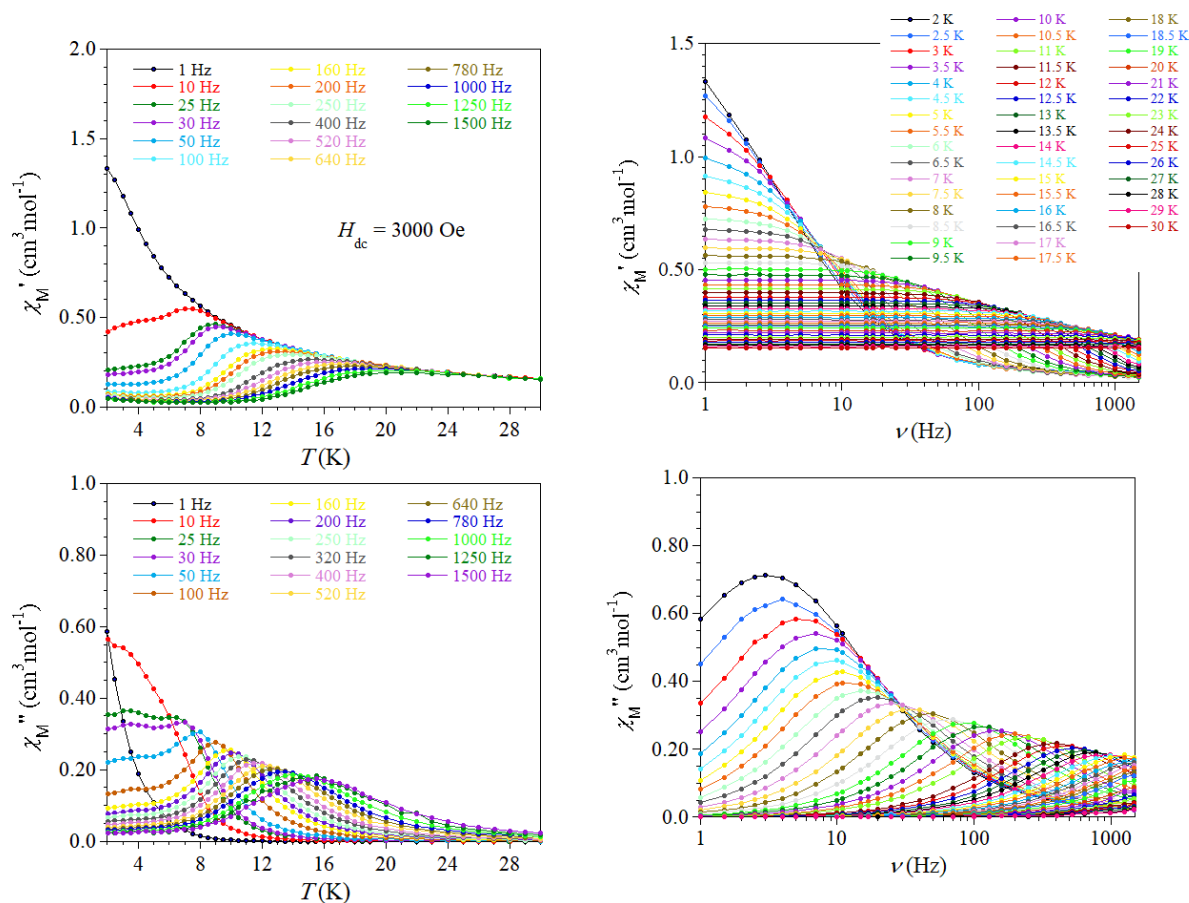

(a)　　　　　　　　　　　　(b)

Figure S4. Compound **1**: (**a**) Frequency dependence of the out-of-phase ac signal (χ_M'') at 5 K with applied fields ranging from 0 and 1 T; (**b**) Field dependence of the relaxation time.

T (K)	τ (s)	α	R²
2	0.051(1)	0.254(4)	0.99968
2.5	0.040(1)	0.239(3)	0.9998
3	0.029(1)	0.208(2)	0.99989
3.5	0.023(1)	0.183(2)	0.9999
4	0.019(1)	0.164(3)	0.99967
4.5	0.016(1)	0.148(5)	0.99924
5	0.014(1)	0.139(1)	0.99869
5.5	0.012(1)	0.125(7)	0.99799
6	0.0095(1)	0.123(8)	0.99777
6.5	0.0074(1)	0.102(1)	0.99764
7	0.0057(1)	0.087(7)	0.99788
7.5	0.0043(1)	0.070(6)	0.9986
8	0.0032(1)	0.058(1)	0.99915
8.5	0.0024(1)	0.048(2)	0.99944
9	0.0018(1)	0.039(4)	0.99971
9.5	0.0014(1)	0.031(4)	0.9998
10	0.0010(1)	0.044(4)	0.99943
10.5	0.000799(1)	0.042(4)	0.99953
11	0.000640(1)	0.034(3)	0.9998
11.5	0.000519(1)	0.030(3)	0.99987
12	0.000415(1)	0.028(3)	0.99988
12.5	0.000347(1)	0.019(2)	0.99996
13	0.000289(1)	0.020(3)	0.99997
13.5	0.000248(1)	0.012(4)	0.99994

14	0.000209(1)	0.018(2)	0.99998
14.5	0.000183(1)	0.012(3)	0.99996
15	0.000155(1)	0.017(4)	0.99995

Figure S5. Frequency and temperature dependence of the in-phase (χ_M') and out-of-phase (χ_M'') ac signals for **1**. AC susceptibilities was recorded in 3 kOe dc field with a 3 Oe ac field with frequencies and temperatures ranging from 1 to 1500 Hz and 2 to 30 K, respectively. Solid lines are guides for the eyes. Relaxation times deduced from $\chi_M'' = f$(Frq) behavior for different temperatures using an extended Debye model are gathered in the table.
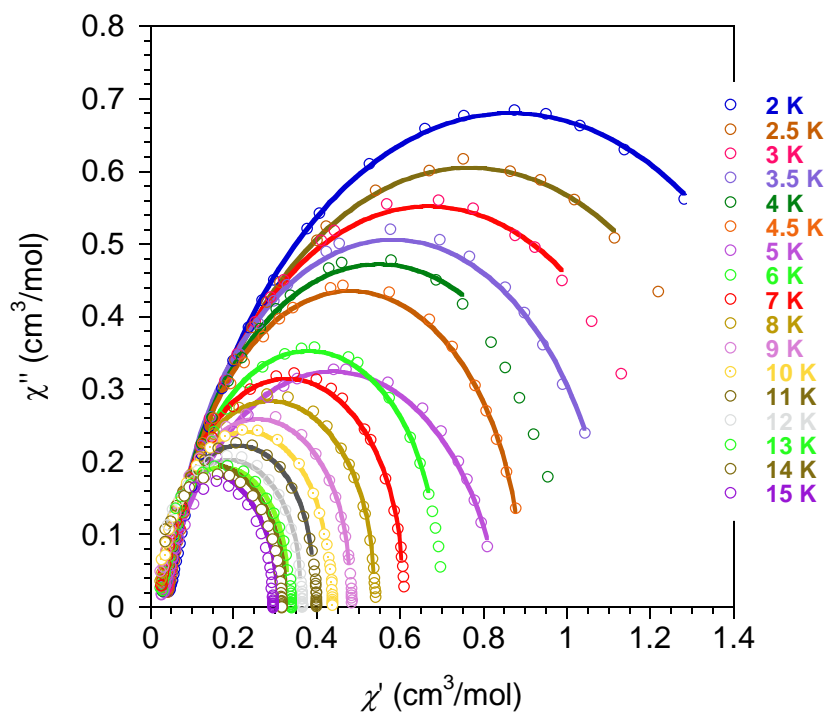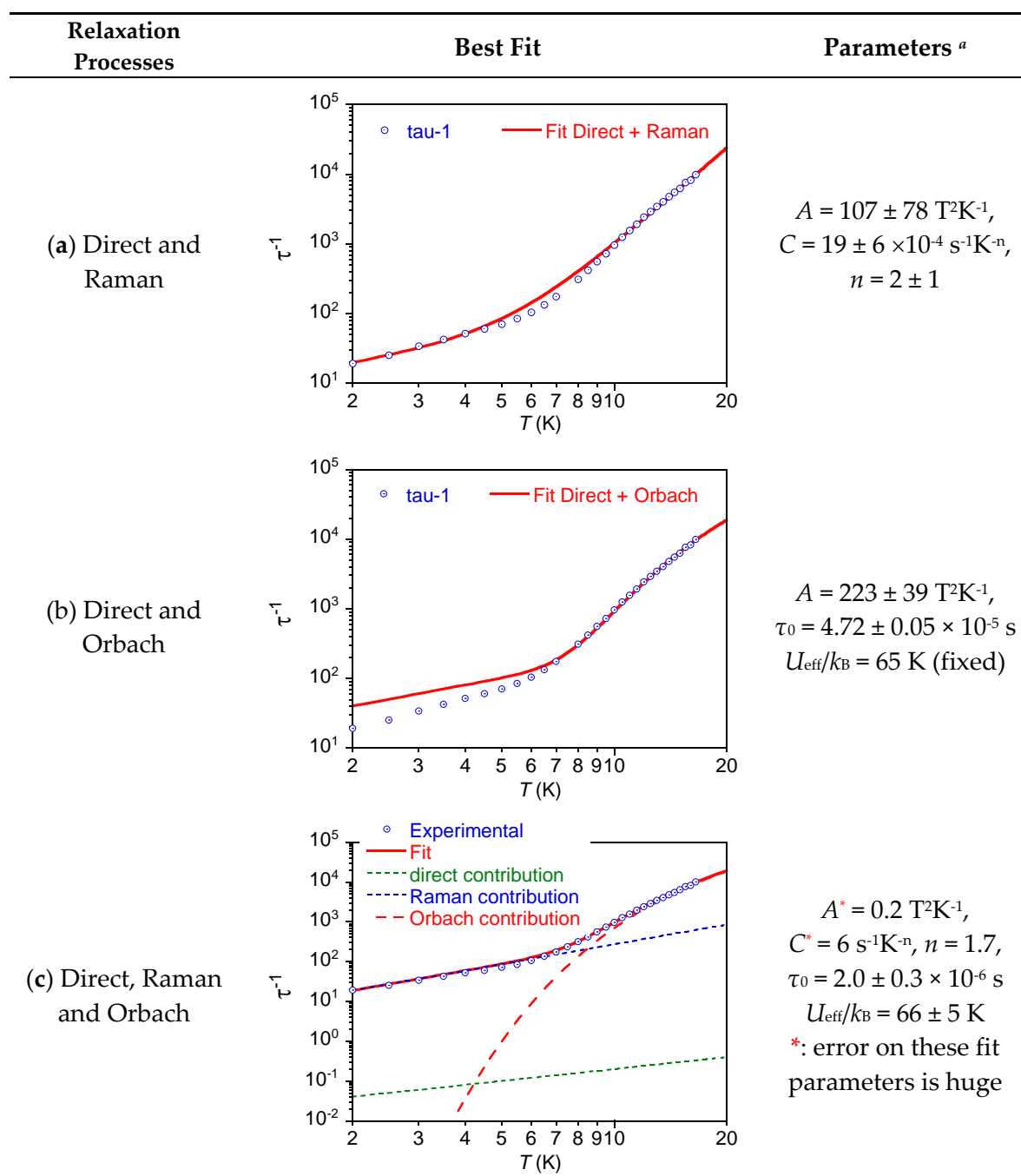
T (K)	χ_T (cm³·mol⁻¹)	χ_S (cm³·mol⁻¹)	α	R²
2	2.482(1)	0.120(1)	0.281(3)	0.99972
2.5	2.051(4)	0.099(1)	0.272(2)	0.99964
3	1.738(3)	0.088(1)	0.253(2)	0.99958
3.5	1.516(2)	0.073(1)	0.251(2)	0.99933
4	1.335(2)	0.066(1)	0.243(3)	0.99884
4.5	1.199(3)	0.056(1)	0.241(4)	0.99765
5	1.081(2)	0.053(2)	0.228(5)	0.99609
5.5	0.985(2)	0.052(2)	0.214(6)	0.99502
6	0.903(2)	0.055(3)	0.190(1)	0.99401
6.5	0.832(2)	0.059(3)	0.158(9)	0.99321
7	0.782(2)	0.050(3)	0.160(1)	0.99680
7.5	0.748(3)	0.040(2)	0.174(7)	0.99235
8	0.688(2)	0.040(2)	0.137(1)	0.99495
8.5	0.647(1)	0.039(2)	0.120(9)	0.99487
9	0.606(1)	0.039(2)	0.095(1)	0.99770
9.5	0.543(4)	0.045(2)	0.045(6)	0.99669
10	0.542(3)	0.043(2)	0.046(6)	0.99825
10.5	0.516(1)	0.047(2)	0.030(5)	0.99796
11	0.493(1)	0.050(3)	0.014(6)	0.99848
11.5	0.472(1)	0.040(2)	0.025(5)	0.99923
12	0.454(1)	0.034(2)	0.039(5)	0.99967
12.5	0.436(1)	0.032(1)	0.033(4)	0.99756
13	0.418(1)	0.032(1)	0.027(8)	0.99970
13.5	0.404(3)	0.032(2)	0.025(4)	0.99964
14	0.389(4)	0.030(2)	0.017(5)	0.99746
14.5	0.376(1)	0.013(6)	0.042(7)	0.99588
15	0.364(1)	0.013(1)	0.038(1)	0.99643
15.5	0.352(1)	0.010(1)	0.040(1)	0.99578
16	0.341(1)	0.016(1)	0.028(1)	0.99987
16.5	0.334(5)	0.010(5)	0.038(7)	0.99967

17	0.322(2)	0.010(6)	0.028(6)

$$\chi'' = (\chi_S - \chi_T)\tan(\frac{\pi\alpha}{2}) + \sqrt{\left[\left(\frac{\chi_S - \chi_T}{2}\right)^2 \left\{\left[tan\left(\frac{\pi\alpha}{2}\right)\right]^2 + 1\right\} - \left(\chi' - \frac{\chi_S - \chi_T}{2}\right)^2\right]} \qquad (1)$$

Figure S6. Cole-Cole ($\chi_M'' = f(\chi_M')$) plots for **1** between 2.5 and 17 K with the best fits to the generalized Debye model (Equation 1) [2] best fit parameters are gathered in the table.

Relaxation Processes	Best Fit	Parameters [a]
(**a**) Direct and Raman		$A = 107 \pm 78$ T^{2}K^{-1}, $C = 19 \pm 6 \times 10^{-4}$ s^{-1}K^{-n}, $n = 2 \pm 1$
(**b**) Direct and Orbach		$A = 223 \pm 39$ T^{2}K^{-1}, $\tau_0 = 4.72 \pm 0.05 \times 10^{-5}$ s $U_{eff}/k_B = 65$ K (fixed)
(**c**) Direct, Raman and Orbach		$A^* = 0.2$ T^{2}K^{-1}, $C^* = 6$ s^{-1}K^{-n}, $n = 1.7$, $\tau_0 = 2.0 \pm 0.3 \times 10^{-6}$ s $U_{eff}/k_B = 66 \pm 5$ K $*$: error on these fit parameters is huge

$$^a: \tau^{-1} = AH^2T + CT^n + \tau_0^{-1}\exp\left(\frac{-U_{eff}}{k_BT}\right)$$

Figure S7. Temperature dependence of τ^{-1} of **1** with the best fit considering (**a**) direct and Raman processes (**b**) direct and Orbach processes, (**c**) Raman, Orbach, and direct processes.
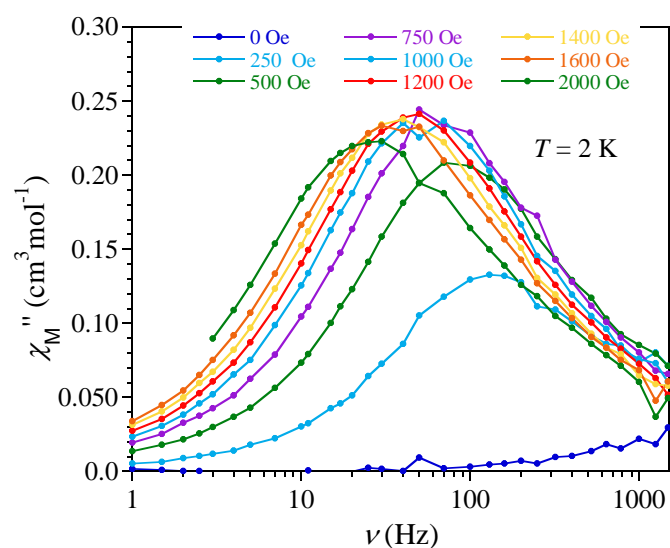
AC Susceptibility Investigations for Na$_9$[Yb(W$_5$O$_{18}$)$_2$]·35H$_2$O, 2:

Figure S8. Temperature dependence of the out-of-phase ac signal (χ_M'') at 2 K for different DC fields. The best compromise between slow relaxation and signal intensity is found for H_{DC} = 1.2 kOe.
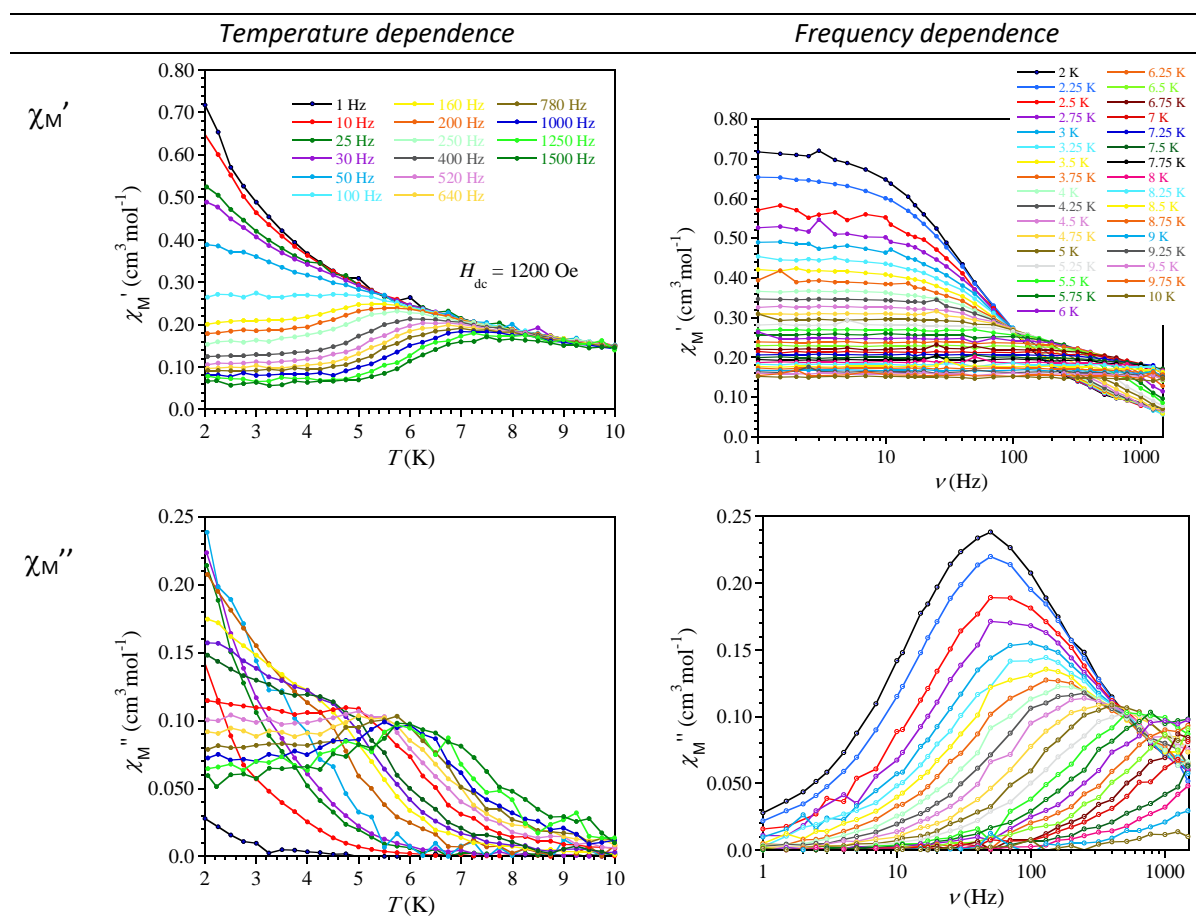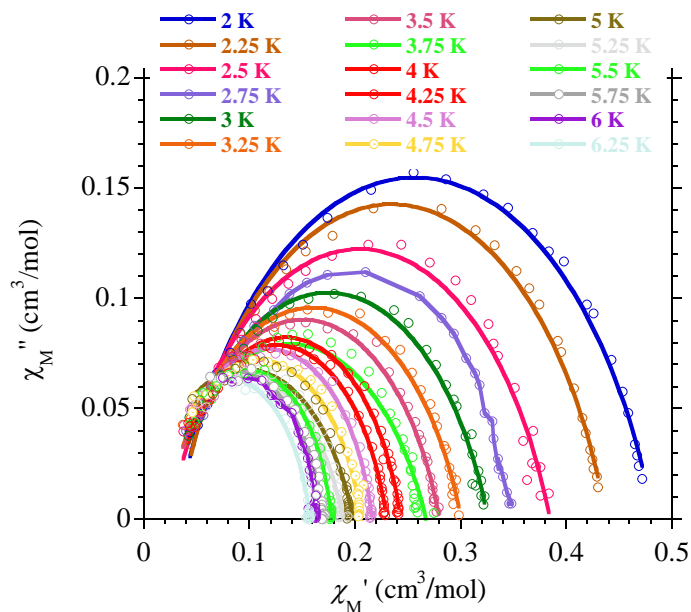

Figure S9. Temperature and frequency dependence of the in-phase (χ') and out-of-phase (χ'') ac susceptibilities recorded at 1.2 kOe dc field with a 3 Oe ac field.

T (K)	χ_T (cm³·mol⁻¹)	χ_S (cm³·mol⁻¹)	α	R^2
2	0.482(1)	0.033(1)	0.229(7)	0.99554
2.25	0.436(1)	0.042(1)	0.188(1)	0.99972
2.5	0.393(3)	0.034(3)	0.233(1)	0.99355
2.75	0.363(2)	0.025(1)	0.259(8)	0.99633
3	0.330(1)	0.026(1)	0.247(6)	0.99856
3.25	0.301(1)	0.034(2)	0.206(9)	0.99848
3.5	0.279(5)	0.032(2)	0.198(3)	0.99829
3.75	0.261(5)	0.032(2)	0.186(9)	0.99701
4	0.245(3)	0.026(1)	0.187(5)	0.99874
4.25	0.230(1)	0.034(2)	0.145(9)	0.99875
4.5	0.217(5)	0.030(2)	0.136(1)	0.99827
4.75	0.208(7)	0.022(2)	0.153(1)	0.99735
5	0.195(2)	0.029(2)	0.099(1)	0.99881
5.25	0.186(4)	0.023(2)	0.105(1)	0.99586
5.5	0.178(4)	0.018(1)	0.108(1)	0.99539
5.75	0.173(6)	0.004(3)	0.133(6)	0.99889
6	0.165(5)	0.004(5)	0.132(18)	0.9982
6.25	0.158(2)	0.021(2)	0.066(8)	0.99963
6.5	0.153(1)	0.011(7)	0.092(2)	0.99856

Figure S10. Cole-Cole ($\chi_M'' = f(\chi_M')$) plots for **2** between 2 and 6.25 K with the best fits to the generalized Debye model (Equation (1)) [2]; best fit parameters are gathered in the table.

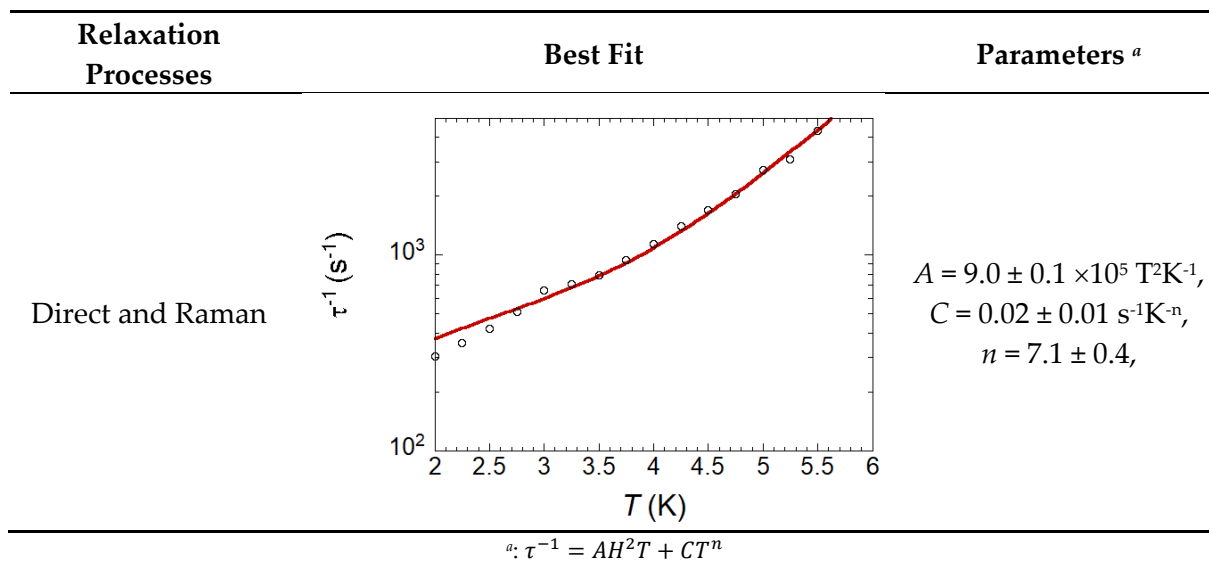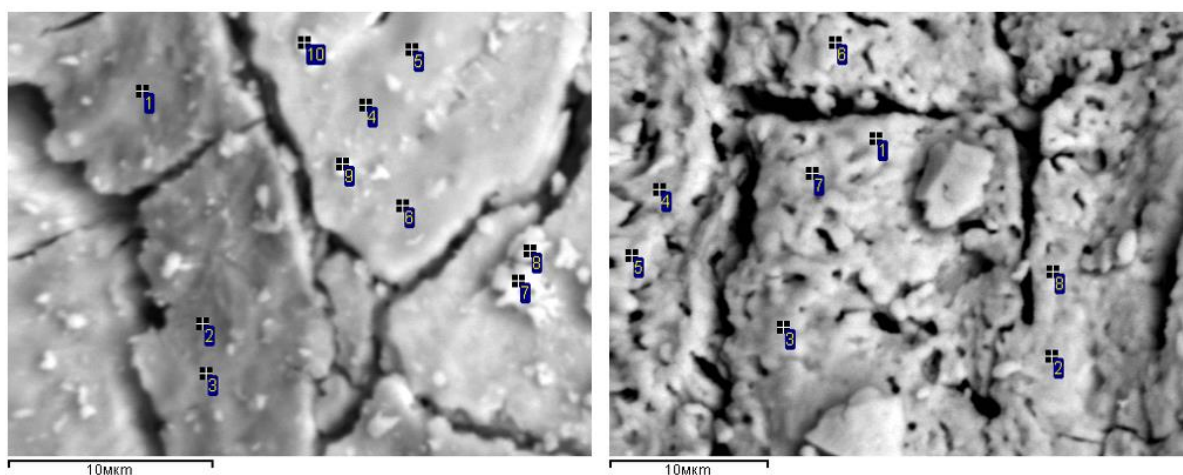| Relaxation Processes	Best Fit	Parameters [a]
Direct and Raman		$A = 9.0 \pm 0.1 \times 10^5$ T^{2}K^{-1}, $C = 0.02 \pm 0.01$ s^{-1}K^{-n}, $n = 7.1 \pm 0.4$,

[a]: $\tau^{-1} = AH^2T + CT^n$

Figure S11. Temperature dependence of τ^{-1} of **2** with the best fit supposing direct and Raman processes.

Atomic ratio of Na, Ln, and W in different points marked on the pictures above- of triturated samples of **1** and **2**.

Points	Salt 1 at. %			Points	Salt 2 at. %		
	Na	**Tm**	**W**		**Na**	**Yb**	**W**
1	16.71	1.89	18.43	1	16.87	1.84	18.29
2	16.69	1.74	18.61	2	16.55	1.92	18.28
3	16.62	1.86	18.16	3	16.73	1.77	18.11
4	16.84	1.75	18.59	4	16.83	1.71	18.62
5	16.92	1.61	18.50	5	16.59	1.89	18.82
6	16.60	1.81	18.36	6	16.63	1.91	18.55
7	16.59	1.94	18.97	7	16.89	1.99	18.78
8	16.70	1.96	19.21	8	16.65	1.85	18.83
9	16.95	1.86	19.41				
10	16.45	1.91	18.88				
Average	16.71	1.83	18.71	Average	16.72	1.86	18.54
Atomic ratio	9.11	1.00	10.21	Atomic ratio	8.99	1.00	9.97

Figure S12. SEM images of the morphology of triturated samples of **1** (*left*) and **2** (*right*). EDX analysis was made in points indicated (see table above).
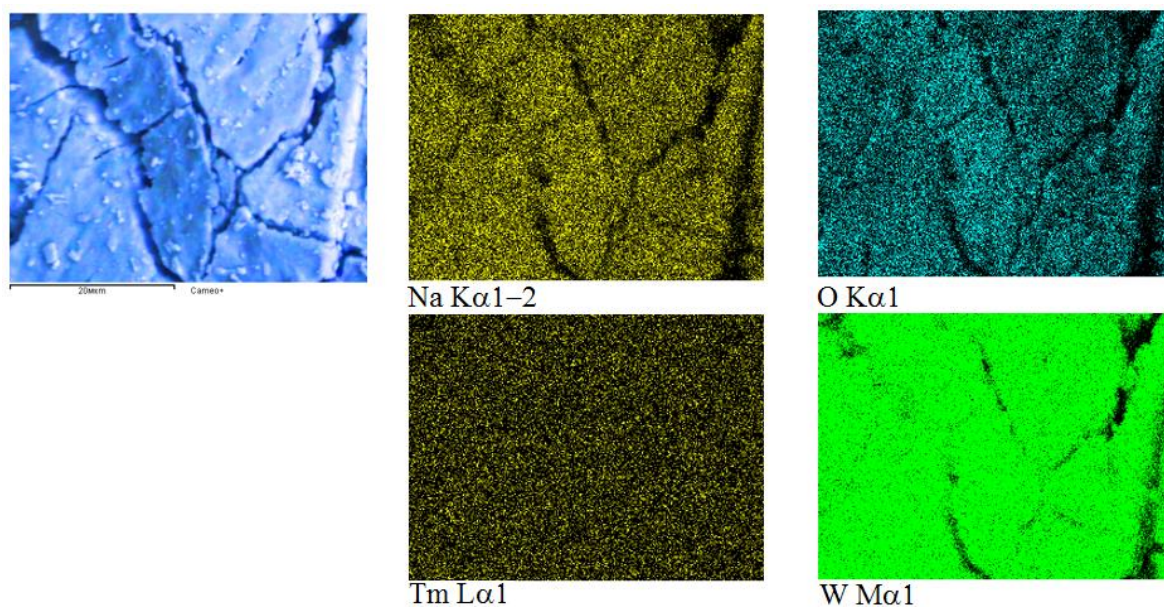
Na Kα1−2

O Kα1

Tm Lα1

W Mα1

Figure S13. SEM images of the powder of **1** in the characteristic X-ray emission.
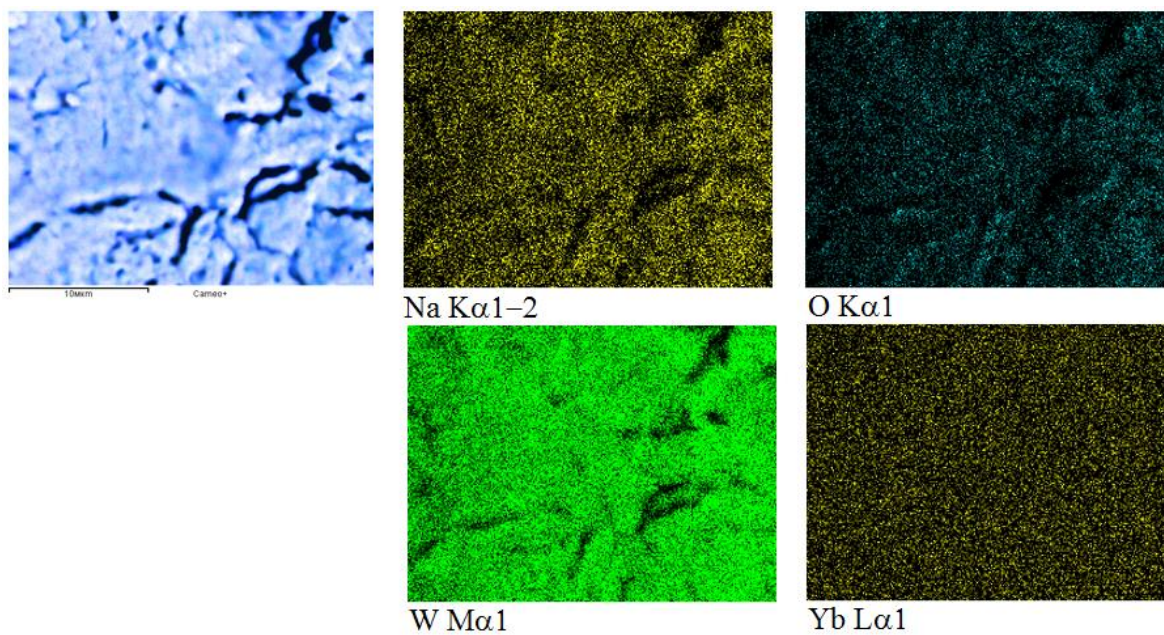
Na Kα1−2

O Kα1

W Mα1

Yb Lα1

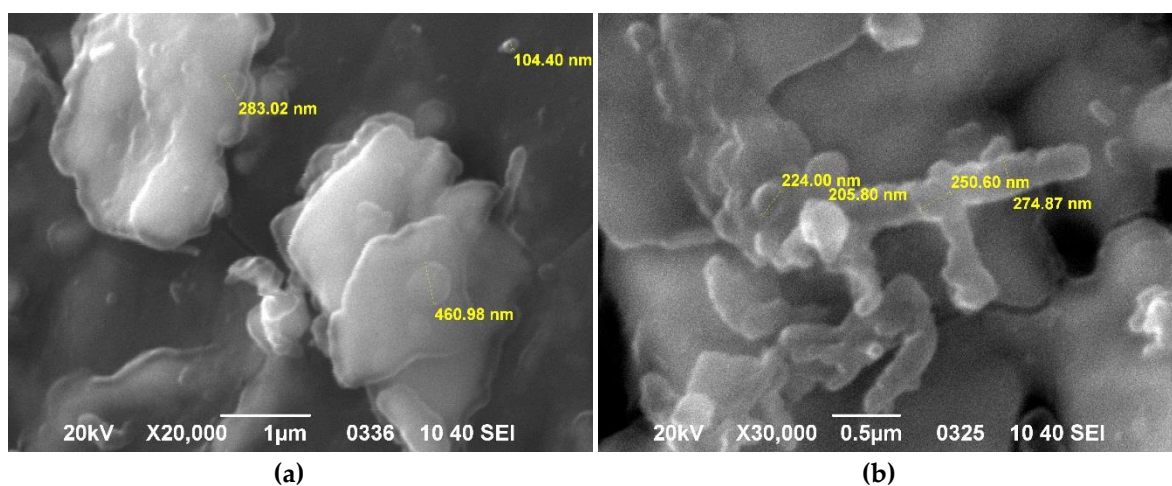**Figure S14.** SEM images of the powder of **2** in the characteristic X-ray emission.

Figure S15. SEM image of the surface of triturated samples of **1** (×20,000 times) (**a**) and **2** (×30,000 times) (**b**).

Table S1. Results of Continuous Shape Measures calculation using SHAPE [3] with the closest geometry for the lanthanide highlighted in blue [4].

Metal center	SAPR	TDD	JBTPR	BTPR
Tm@**1**	0.066	2.458	2.757	2.246
Yb@**2**	0.063	2.453	2.802	2.250

Geometry	Point symmetry
SAPR: Square antiprism	D_{4d}
TDD: Triangular dodecahedron	D_{2d}
JBTPR: Biaugmented trigonal prism J50	C_{2v}
BTPR: Biaugmented trigonal prism	C_{2v}

Table S2. SF-CASSCF and SO-CASSCF energies for the [Ln(W₅O₁₈)₂]⁹⁻ complexes. The Spin-Free (SF) states are given according to their spin multiplicity and the Spin-Orbit (SO) states are decomposed in terms of M_J, with the pseudo C_4 axis as quantification axis.

SF				SO			
Tm(III)		**Yb(III)**		**Tm(III)**		**Yb(III)**	
	ΔE		**ΔE**	**ΔE**	**comp**	**ΔE**	**comp**
triplet	0	doublet	0	0	100% ±6	0	97% ±5/2
	0.5		44	0		0	
	310		93	319	44% ±5 ; 23% ±3	65	97% ±7/2
	328		97	320	49% ±5 ; 28% ±3	65	
	355		383	335	42% 5 ; 20% ±2	254	99% ±3/2
	362		389	335	41% 5 ; 32% ±2	254	
	372		396	352	68% ±3	363	99% ±1/2
	387			363	50% ±2; 26% ±4	363	
	389			369	42% ±4; 38% ±1	10343	
	406			380	48% ±4; 23% ±2	10343	
	408			381	42% ±4;32% ±1		
	8204			387	79% ±2		
	8215			389	65% 0		
	8243			6948			
	8314			7026			
	8325						
	8337						
	8338						
singlet	9159						
	9252						
	9260						
	9327						
	9333						
	9497						
	9502						
	9575						
	9585						

Table S3. *g* factors of for the [Ln(W₅O₁₈)₂]⁹⁻ complexes deduced from SO-CASSCF calculations. For the Tm(III) complex, **1**, the *g* value is deduced from non Kramers doublet; the corresponding principal axis has a projection ω_z on the *z* axis.

Tm(III)			Yb(III)			
NKD	**g**	**ω_z**	**KD**	**g_x**	**g_y**	**g_z**
1-2	14.0	1.0	KD1	0.2	0.4	5.9
3-4	11.8	0.72	KD2	0.1	0.1	8.0
5-6	9.1	0.67	KD3	0.1	0.8	3.4
8-9	4.9	0.56	KD4	4.1	5.0	1.1
10-11	11.2	0.53				
12-13	13.0	0.09				

Table S4. Crystal field and strength parameters (in cm⁻¹) for the [Ln(W₅O₁₈)₂]⁹⁻ complexes deduced from SO-CASSCF calculations.

	Tm(III)	Yb(III)		Tm(III)	Yb(III)
B_0^2	-552	-530	S [a]	218	204
B_1^2	51	35	S^2 [b]	250	238
B_2^2	44	13	S^4	259	243
B_0^4	-775	-728	S^6	113	96
B_1^4	13	17	S_0 [c]	374	352
B_2^4	14	10	S_1	34	24
B_3^4	22	10	S_2	29	10
B_4^4	44	40	S_3	11	6
B_0^6	397	337	S_4	31	29
B_1^6	18	13	S_5	2	3
B_2^6	5	3	S_6	3	2
B_3^6	12	11			
B_4^6	59	56			
B_5^6	6	8			
B_6^6	9	7			

[a] $S = \left[\frac{1}{3}\sum_{k=2,4,6}\frac{1}{2k+1}\sum_{q=-k}^{k}\left|B_q^k\right|^2\right]^{1/2}$; [b] $S^k = \left[\frac{1}{2k+1}\sum_{q=-k}^{k}\left|B_q^k\right|^2\right]^{1/2}$; [c] $S_q = \left[\frac{1}{3}\sum_{k=2,4,6}\frac{1}{2k+1}\left|B_q^k\right|^2\right]^{1/2}$

References

1. Cumby, J.; Attfield, J.P. Ellipsoidal analysis of coordination polyhedral. *Nature Comm.* **2017**, *8*, 14235.
2. Cole, K.S.; Cole, R.H. Dispersion and Absorption in Dielectrics I. Alternating Current Characteristics. *J. Chem. Phys.* **1941**, *9*, 341, doi:10.1063/1.1750906.
3. Llunell, M.; Casanova, D.; Cirera, J.; Alemany, P.; Alvarez, S. SHAPE: Program for the stereochemical analysis of molecular fragments by means of continuous shape measures and associated tools; University of Barcelona: Barcelona, Spain, 2013.
4. Casanova, D.; Alemany, P.; Bofill, J.M.; Alvarez, S. Shape and Symmetry of Heptacoordinate Transition-Metal Complexes: Structural Trends. *Chem. Eur. J.* **2003**, *9*, 1281, doi:10.1002/chem.200390145.